Implications of the Reactive Thiol and the Proximal Non-Proline *cis*-Peptide Bond in the Structure and Function of *Vibrio harveyi* Luciferase[†,‡]

Leo Yen-Cheng Lin,[§] Traian Sulea,[||] Rose Szittner,[§] Christine Kor,[§] Enrico O. Purisima,[||] and Edward A. Meighen*[,§]

Department of Biochemistry, McGill University, 3655 Promenade Sir William Osler, Montreal, Quebec, Canada H3G 1Y6, and Biotechnology Research Institute, National Research Council of Canada, 6100 Royalmount Avenue, Montreal, Quebec, Canada H4P 2R2

Received April 19, 2002; Revised Manuscript Received May 30, 2002

ABSTRACT: The role of a highly reactive cysteine residue, Cys106, in *Vibrio harveyi* luciferase in modulating the substrate−enzyme interactions and in turn affecting the enzyme activity has been extensively investigated over the past three decades. Replacing Cys106 with valine dramatically hinders the ability of luciferase to stabilize the C4a-hydroperoxyflavin intermediate [Abu-Soud, H. M., Clark, A. C., Francisco, W. A., Baldwin, T. O., and Raushel, F. M. (1993) *J. Biol. Chem. 268*, 7699−7706] and consume aldehyde substrate [Xi, L., Cho, K.-W., Herndon, M. E., and Tu, S.-C. (1990) *J. Biol. Chem. 265*, 4200−4203], therefore markedly decreasing enzyme activity. On the basis of the structure−activity relationship of flavin analogues and the location of the phosphate binding site of flavin mononucleotide (FMN) coupled with molecular modeling, the functional part of the isoalloxazine ring of FMN, the thiol side chain of Cys106, the methyl group of Ala75, and the unique non-prolyl *cis*-peptide bond between Ala74 and Ala75 were found to be closely packed [Lin, L. Y., Sulea, T., Szittner, R., Vassilyev, V., Purisima, E. O., and Meighen, E. A. (2001) *Protein Sci. 10*, 1563−1571]. Here, by mutating Ala75 to Gly, we restored key wild-type properties to the C106V mutant, in particular, high enzyme activity and a stable C4a-hydroperoxyflavin intermediate, demonstrating that the primary reason for the dark phenotype of the C106V mutant was the unfavorable steric interaction between Val106 and Ala75 side chains, which could in turn disturb the *cis*-oriented amide linkage of Ala74 and Ala75. Moreover, significant red shifts in light emission of 3−10 nm were measured for luciferases carrying Val106 with the spectrum of the double mutant C106V/A75G now red shifted to that of *Photobacterium phosphoreum* luciferase, which also has Val and Gly at positions 106 and 75, respectively. These results strengthen the validity of the binding geometry of the modeled flavin with the *re*-face of the pyrimidine end of the isoalloxazine ring next to Cys106 and implicate the Ala74−Ala75 *cis*-peptide as a key component in the bioluminescence reaction.

Bacterial luciferase catalyzes the oxidation of $FMNH_2$ and fatty aldehyde, leading to the reduction of molecular oxygen to water and the dissipation of excess energy in the form of blue-green light (∼490 nm). All bacterial luciferases are heterodimers containing homologous subunits designated α and β. The active site of the luciferase from *Vibrio harveyi* bacteria is believed to lie in a spacious cavity located at the center of the $(\beta/\alpha)_8$ barrel structure of the α subunit in the crystal structure (*1*). A phosphate binding site corresponding to the phosphate group of $FMNH_2$[1] has been identified in this putative active site cavity (*2*−*4*). We have recently proposed the binding geometry of flavin mononucleotide in the active site of luciferase by using the phosphate binding site and the structural requirements of the flavin side chain as guiding pharmacophores in molecular modeling (*4*). Interestingly, the catalytic C4a site of the isoalloxazine moiety of the modeled flavin mononucleotide was positioned right above a rare non-prolyl *cis*-amide linkage connecting Ala74 and Ala75 (*4*). Unusual structural elements such as the non-prolyl *cis*-peptide bonds have been suspected of playing key roles in the function and structure of enzymes; in addition, aliphatic amino acids in a *cis*-peptide arrangement are also the rarest type of non-prolyl *cis*-peptide linkages (*5*). Tightly packed against the *re*-face of the pyrimidine portion of flavin and in the proximity of the methyl side chain of Ala75 is the reactive thiol of Cys106 (*4*). The role of the reactive thiol of Cys106 in *V. harveyi* luciferase has been extensively explored in the past three decades (*6*−*18*). In particular, the mutation of Cys106 to valine has been shown to substantially reduce luciferase activity by destabilizing the C4a-hydroperoxyflavin intermediate formed in the reaction (*6*) and hindering aldehyde consumption (*6*, *18*). As homologous luciferases from other species, including those from *Vibrio (Photobacterium) fischeri*, *Photobacterium phosphoreum*, and *Photobacterium leiognathi*, have valine at position 106 (*19*) and also have

[†] Supported by Grant MT4314 from the Canadian Institutes of Health Research (CIHR). L.Y.-C.L. was a recipient of the Natural Science and Engineering Research Council of Canada (NSERC) postgraduate scholarship and the 2002 Marlene DeLuca prize.

[‡] This is National Research Council of Canada publication 44944.

* To whom correspondence should be addressed. Telephone: (514) 398-7272. Fax: (514) 398-7384. E-mail: meighen@med.mcgill.ca.

[§] McGill University.

[||] National Research Council of Canada.

[1] Abbreviations: FMN, flavin mononucleotide; $FMNH_2$, reduced FMN; *Vh*, *Vibrio harveyi*.

10.1021/bi020295o CCC: $22.00 © 2002 American Chemical Society
Published on Web 07/11/2002

glycine rather than alanine at position 75, the significant loss of activity may reflect the importance of side chain packing in not disturbing the nearby non-prolyl *cis*-peptide linkage and its interaction with the isoalloxazine ring in the proposed flavin−luciferase binary complex model (*4*). Here, we investigate the Cys106 → valine mutation in combination with mutation of the proximal Ala75 of the *cis*-bond to confirm a direct structural interaction between the reactive thiol and the methyl side chain of Ala75 in the active site of *V. harveyi* luciferase. These results not only unveil the basis for the C106V dark phenotype but also highlight the validity of the location and geometry of the modeled flavin in the active site of bacterial luciferase (*4*) and further suggest a potential role of the non-prolyl *cis*-peptide bond in the bioluminescence reaction.

EXPERIMENTAL PROCEDURES

Chemicals. The concentration of flavin mononucleotide (FMN) was determined using an extinction coefficient of 12 200 M^{-1} cm^{-1} at 450 nm. β-Mercaptoethanol and FMN were obtained from Sigma. The phosphate buffer solution (pH 7.0) was prepared by mixing appropriate amounts of NaH_2PO_4 and K_2HPO_4 obtained from Baker. Sodium dithionite was purchased from Fisher. Octanal, nonanal, decanal, undecanal, and dodecanal were all purchased from Aldrich.

Site-Directed Mutagenesis. The *V. harveyi lux*AB gene in M13 was mutated using the Muta-Gene M13 In Vitro Mutagenesis kit from Bio-Rad. The codon for alanine at position 75 (GCT) was changed to GGG (Gly), and the codon for cysteine at position 106 (TGT) was changed to GTT (Val). The mutated codons were confirmed by DNA sequencing using the Sequenase DNA Sequencing Kit (version 2) from U.S. Biochemical. The mutated *lux*AB was transferred to the pT7-5 expression vector, and the sequence was reconfirmed as described above.

Expression and Enzyme Purification. Each of the pT7-5 plasmids containing the mutated *V. harveyi lux*AB genes was transformed into *Escherichia coli* BL21 whose chromosomal DNA contains the IPTG (isopropyl β-D-thiogalactopyranoside)-inducible T7 RNA polymerase. The cells were grown in the appropriate medium containing 50 μg/mL ampicillin at 30 °C, and IPTG was added to a final concentration of 0.6 mM when the cell density reached an OD_{660} of 1.2−1.3. Following the induction with IPTG, the cell culture was allowed to grow for 1 h before luciferase extraction took place. The *P. phosphoreum* luciferase was prepared from the native cells grown under the conditions described by Hastings et al. (*20*). Cells harboring the luciferases were harvested, centrifuged, and resuspended in 10% of the original culture volume of 50 mM phosphate buffer (pH 7.0) and 20 mM β-mercaptoethanol before lysis by ultrasonication. Purification was performed according to previous methods (*21*). Protein concentrations were first estimated using the Bio-Rad protein determination kit with BSA (bovine serum albumin) as a standard. More accurate protein concentrations were determined spectrophotometrically using the protein extinction coefficients calculated using Gill and von Hippel's method (*22*).

Measurement of Luminescence Intensity. Three different techniques are employed, depending on the kinetic parameter in question. They are the standard flavin injection assay, the sodium dithionite assay, and the double-injection assay. The activities of luciferases, including mutants and the wild type, were determined using the standard flavin injection assay in which 1 mL of platinum−hydrogen gas-reduced 50 μM flavin mononucleotide ($FMNH_2$) was rapidly injected into 1 mL of assay buffer [50 mM phosphate and 0.2% bovine serum albumin (pH 7.0)] containing aldehyde (0.001% for measuring the specific activities and the rates of luminescence decay) and luciferase. The rate of luminescence decay ($k_L = 0.69/t_{1/2}$) was determined from the time ($t_{1/2}$) it took for the light intensity to decay from 80 to 40% of the maximum light intensity. The binding affinity of luciferase for $FMNH_2$ ($K_D = K_M$) was determined using the dithionite assay (*23*) in which 1 mL of 0.1% decanal (v/v in water) was injected into 1 mL of assay mixture (pH 7.0) containing luciferase, FMN, 0.2 mg of sodium dithionite, 0.025 M β-mercaptoethanol, and 50 mM phosphate. The stability of the C4a-hydroperoxyflavin intermediate was determined by the double-injection assay (*24*), in which 1 mL of platinum−hydrogen gas-reduced 50 μM flavin mononucleotide was first injected into 1 mL of assay mixture (pH 7.0) containing luciferase, 0.2% bovine serum albumin, and 50 mM phosphate, followed by injection of 1 mL of 0.1% decanal (v/v in water) at different time points.

Luminescence Wavelength Scan. The emission wavelength spectra were scanned with a Hitachi F-3010 spectrofluorometer using the following settings: internal shutter closed to block the xenon lamp from exciting the sample, wavelength dispersion for emission band-pass set at 5 nm, scan speed of 600 nm/min between 420 and 550 nm, and sample chamber temperature controlled at 23 °C. Luminescence was generated from a 1 mL mixture containing 50 mM phosphate buffer (pH 7), 0.2% bovine serum albumin, 5 mM β-mercaptoethanol, 0.1 mM decanal, 5 μM FMN, 1 mM β-nicotinamide adenine dinucleotide (NAD), 5 mM glucose 6-phosphate, 0.2 unit of glucose-6-phosphate dehydrogenase, approximately 50 μg of ≥90% pure luciferase (note that a much larger amount of pure C106V luciferase, approximately 1 mg, was used in this assay protocol to produce luminescence with a high signal-to-noise ratio), and a fixed amount of FMN reductase. The mixture was mixed with an in-curvet magnetic stir bar using the magnetic stirring device built into the spectrofluorometer. Light intensity remained constant over the period of the scan.

Scheme 1: Key Intermediates in the Bacterial Luminescence Reaction

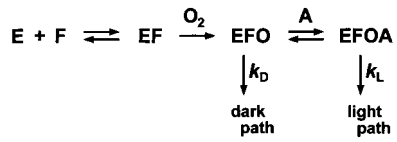

RESULTS

Single-Turnover Assay. The reaction pathway (Scheme 1), formulated by Hastings and Gibson (*25*), outlines the basic intermediates involved in the reaction pathway catalyzed by bacterial luciferase. A unique intermediate in the pathway is the luciferase-bound C4a-hydroperoxyflavin (EFO), formed upon the reaction of reduced flavin mononucleotide (F) and molecular oxygen (O_2). In the presence of aldehyde (A), the C4a-hydroperoxyflavin intermediate interacts reversibly with

Table 1: Relative Specific Activities of Luciferase Mutants Compared to That of the Wild Type with Different Aldehydes[a]

mutant	octanal	nonanal	decanal	undecanal	dodecanal
A75G	90	90	80	100	90
C106V	1	2	1	2	3
A75G/C106V	60	80	50	80	80

[a] The specific activities of wild-type luciferase with octanal, nonanal, decanal, undecanal, and dodecanal were 7.7×10^{12}, 5.6×10^{13}, 5.2×10^{13}, 8.8×10^{12}, and 6.7×10^{12} quanta s^{-1} mg^{-1}, respectively.

Table 2: Rates of Luminescence Decay of Wild-Type and Mutant Luciferases with Different Aldehydes[a]

	k_L (min^{-1})				
	octanal	nonanal	decanal	undecanal	dodecanal
wild type	2.7	18.9	15.4	3.4	2.8
A75G	3.7	27.2	22.7	5.7	4.0
C106V	68.2	51.3	60.3	24.9	11.2
A75G/C106V	5.7	19.1	19.5	4.2	2.9

[a] The decay rate ($k_L = \ln 2/t_{1/2}$) was calculated from the time it took luminescence to decay from 80 to 40% of maximum light intensity.

aldehyde to form the stable EFOA complex that will decay with a rate constant, k_L, to emit light. However, in the absence of aldehyde, the EFO intermediate degrades with a decay rate of k_D, through a dark pathway. The turnover of the luciferase-bound C4a-hydroperoxyflavin (EFO) is unusual in that its decay through either the dark or light pathway is much slower than the rate of chemical oxidation of free $FMNH_2$. Consequently, bacterial luciferase catalyzes only one cycle of the reaction upon rapidly mixing the enzyme and the reactants ($FMNH_2$, fatty aldehyde, and O_2), with the initial maximum light intensity (I_o) reflecting the activity of luciferase and the decay of luminescence reflecting k_L.

Specific Activities of Luciferase Mutants. Table 1 compares the specific activities of mutants with respect to the wild-type enzyme for different aliphatic aldehydes. The activity is maintained at the wild-type level (80−100% with different aldehydes) after the removal of the methyl side chain of the second alanine in the *cis*-peptide bond in the mutant, A75G. Replacing Cys106 with valine dramatically decreases the activity as observed previously (*6*, *18*) with C106V yielding only 1−3% of the wild-type luciferase activity. However, activity can almost be fully recovered in the C106V mutant by introduction of the A75G mutation with the double mutant A75G/C106V having activities close to those of the wild-type luciferase (50−80%). This result suggests that the steric packing of these two residues was critical in determining the functional properties of luciferase. Consequently, other relevant kinetic parameters of these mutants were further investigated.

Luminescence Decay and Light Yield. The rate constant for luminescence decay (k_L) reflects the rate of turnover of luciferase in the light pathway. As the enzyme undergoes a single catalytic cycle, the light or quantum yield can be deduced by integrating the light intensity produced during the reaction, which is equal to I_o/k_L. Table 2 shows that the rate constants for luminescence decay of C106V with different aldehydes are significantly increased over those of the wild-type luciferase. In contrast, the rate constants for luminescence decay for mutants, A75G and A75G/C106V, are very similar to those of the wild-type enzyme. These

Table 3: Relative Luminescence Light Yield (%) of Luciferase Mutants[a]

mutant	octanal	nonanal	decanal	undecanal	dodecanal
A75G	70	60	50	60	60
C106V	0.1	0.7	0.2	0.3	0.6
A75G/C106V	30	80	40	60	80

[a] The light yields were calculated by multiplying the specific activities (Table 1) and the $t_{1/2}$ values (Table 2), and expressed as the percentage relative to that of wild-type luciferase.

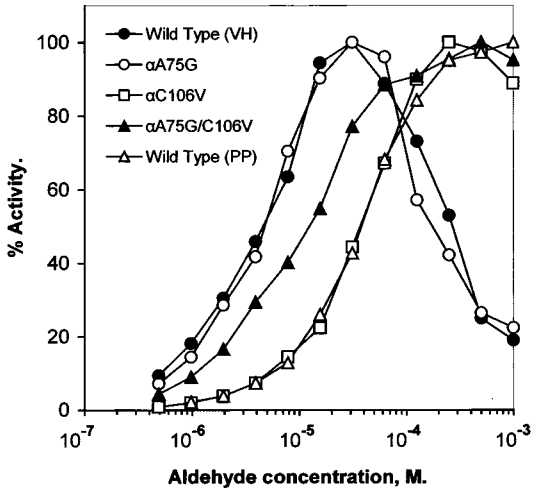

FIGURE 1: Luminescent light intensity as a function of decanal concentration determined for mutant and wild-type luciferases. The % activity on the *y*-axis denotes the percentage of the maximum luminescent light intensity determined for each luciferase.

results show that the removal of the methyl group from Ala75 in the mutant, A75G, is able to compensate for the replacement of Cys106 with the larger valine residue in the C106V mutant. By combination of the activity (I_o) and the rate constants for luminescence decay (k_L) with the respective aldehydes, the relative amount of light produced in one single turnover was calculated. Table 3 shows that the quantum yield for the C106V mutant is very low (0.1−0.6%) but can be restored by introduction of the A75G mutation to levels (30−80%) comparable to those of the wild type.

Binding of $FMNH_2$ and Aldehyde. Substrate binding assays were carried out to explore the possibility that weak interactions with the substrates resulted in the low activity and the low quantum yield of the C106V mutant. The dissociation constants ($K_D = K_M$) of A75G and A75G/C106V for $FMNH_2$, determined using the dithionite assay (*23*), were 3 and 2 μM, respectively, and were slightly weaker than that for C106V, 0.7 μM, which is the same as that of the wild type. Although the thiol side chain of Cys106 is in van der Waals contact with the *re*-face of the isoalloxazine chromophore and the Ala74−Ala75 *cis*-amide establishes hydrogen bonds with the C4 carbonyl oxygen and N5 hydrogen in our luciferase−flavin mononucleotide binary complex model (*4*), this result indicates that the V106↔A75 steric interaction does not affect the affinity of luciferase for $FMNH_2$. Standard $FMNH_2$ injection assays performed at various aldehyde (decanal) concentrations showed that both the *Vh* wild type and the A75G mutant reached their maximum light intensity at the same aldehyde concentration (~30 μM) and were inhibited at higher aldehyde concentrations (Figure 1). In contrast, the C106V mutant required

aldehyde concentrations of ~200 μM to reach maximum luminescence and was not inhibited at aldehyde concentrations up to 1 mM, similar to the properties of *P. phosphoreum* luciferase, which has valine at position 106. The A75G/C106V double mutant had aldehyde binding similar to that of the *V. harveyi* wild-type luciferase, reaching a maximum at 50 μM decanal, but unlike the *Vh* wild-type luciferase was not inhibited at high decanal concentrations. These results clearly distinguish aldehyde inhibition from the rescued properties and associate it directly with Cys106, consistent with the proposal that it is specifically responsible for aldehyde inhibition in *V. harveyi* luciferase (*12*). This inhibition may reflect the high nucleophilicity of the sulfhydryl of Cys106 as it appears to be the only thiol side chain among the 14 cysteine residues in *V. harveyi* luciferase that couples with various chemical-modifying agents (*11*, *13*−*17*). Studies on the mode of substrate inhibition of *V. harveyi* luciferase have suggested two different modes of fatty aldehyde binding to luciferase with one mode being the formation of the active ternary complex (EFOA) which is productive in light emission, and the second mode being the formation of a dead end complex near Cys106 blocking $FMNH_2$ binding at high aldehyde concentrations (*6*, *12*, *26*, *27*). These two aldehyde binding modes are in agreement with our model, in which the isoalloxazine moiety of flavin is in the proximity of the thiol group of Cys106, creating a tunnel-shaped cavity for aldehyde entry on the *si*-face of the flavin isoalloxazine (*4*).

C4a-Hydroperoxyflavin Intermediate Stability. In the absence of aldehyde substrate (A), the luciferase-bound C4a-hydroperoxyflavin intermediate (EFO) degrades through a dark pathway, giving no light (Scheme 1). By injecting the aldehyde (A) at different time points after the formation of the luciferase−C4a-hydroperoxyflavin intermediate complex (EFO), we can determine the level of the active C4a-hydroperoxyflavin intermediate and therefore its decay rate. Figure 2 shows that the C4a-hydroperoxyflavin intermediates of the *Vh* wild-type luciferase and the A75G mutant are very stable. In contrast, the EFO intermediate of the C106V mutant (not shown) decays so rapidly that no significant level of EFO could be detected beyond the first second, and therefore, the decay pattern could not be accurately determined. Rapid-mixing techniques applied by other workers have shown that the half-time for the disintegration of the C106V-bound EFO ranged between 50 (*6*) and 160 ms (*18*), far faster than could be detected by the current instrumentation. In contrast, the decay of the EFO intermediate of the double mutant A75G/C106V could be readily detected, showing that the removal of the methyl group from Ala75 in the *cis*-peptide bond results in recovery of the stability of the C4a-hydroperoxyflavin intermediate lost in the single C106V mutant. Although the decay rate is still faster than that of the *Vh* wild-type luciferase, it is interesting to note that the double mutant has a decay rate in the dark pathway very similar to that of *P. phosphoreum* luciferase, which also has valine and glycine at positions 106 and 75, respectively. Clearly, the relationship of the side chains of these two residues plays an important role in the stability of the C4a-hydroperoxyflavin intermediate, providing strong experimental evidence validating our luciferase−flavin mononucleotide binary complex model (*4*). Steric repulsions between these two side chains in the C106V mutant clearly cause a conformational change in the EFO complex that destabilizes the C4a-hydroperoxyflavin intermediate causing it to decay rapidly.

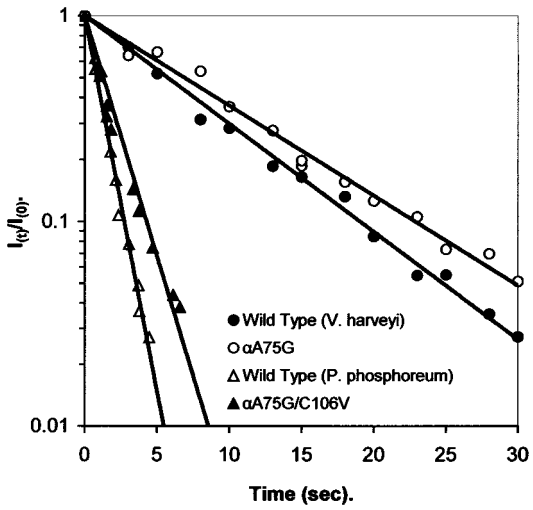

FIGURE 2: Decay of the enzyme−flavin−oxygen (EFO) intermediate as a function of time with mutant and wild-type luciferases. The decay of the *Vh* α-C106V-bound EFO intermediate was so rapid ($t_{1/2}$ < 200 ms) that accurate data could not be recorded. Light intensities were measured using the double-injection assay described in Experimental Procedures. The plotted times were the intervals between the injections of the $FMNH_2$ and decanal solutions. $I_{(t)}/I_{(0)}$ on the *y*-axis is the ratio of the light intensity obtained at a given time interval, $I_{(t)}$, divided by the light intensity obtained when both $FMNH_2$ and decanal solutions were added simultaneously, $I_{(0)}$.

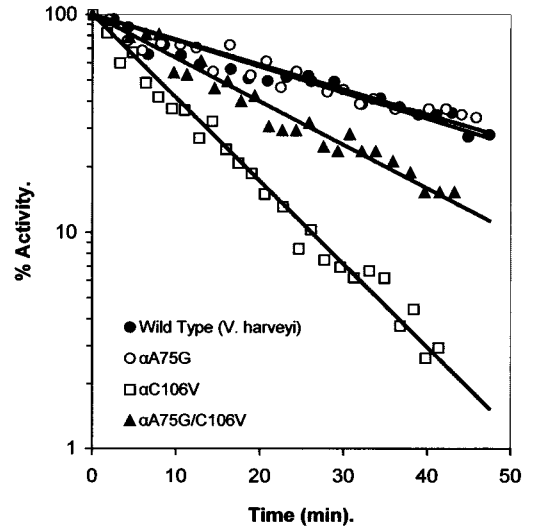

FIGURE 3: Thermal stabilities of the wild-type and mutant luciferases. The luciferases were incubated in 50 mM phosphate (pH 7) and 0.2% bovine serum albumin at 40 °C, and the standard flavin injection assay was performed with aliquots at the designated time points.

Thermal Stability. As the side chains of residues 75 and 106 are in the proximity of the crystal structure, the effect of those point mutations on the protein structural integrity was investigated by assaying their stabilities against heat. Figure 3 shows that A75G and the wild type have identical rates of thermal inactivation (at 40 °C), suggesting that the three-dimensional organization of luciferase is maintained after the removal of the methyl group. The mutant, C106V, is more thermally labile than the wild-type luciferase, indicating some degree of change in structural integrity.

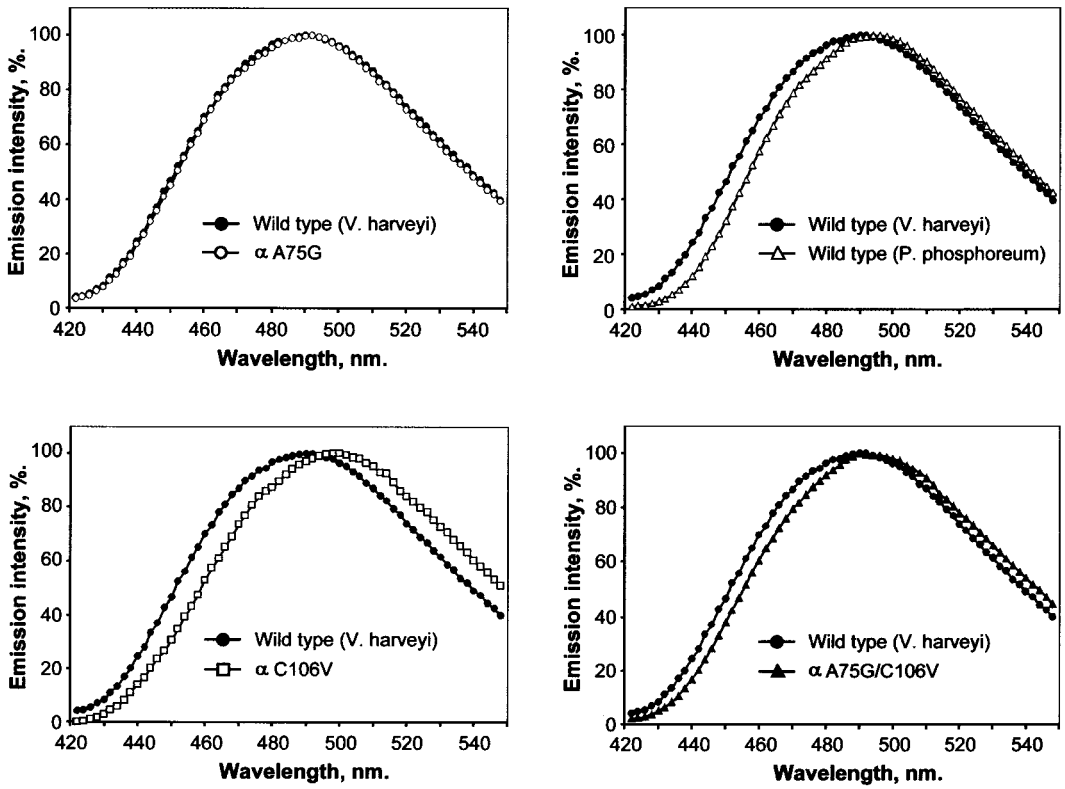

FIGURE 4: Luminescence emission wavelength scans of *V. harveyi* wild-type and mutant luciferases. A large red shift can be observed for the C106V mutant, while a smaller shift (~3−5 nm) was observed for the A75G/C106V double mutant compared to that of wild-type luciferase. The emission spectra of A75G and the wild type were identical as their scan lines overlap.

Addition of the A75G mutation to C106V restores much of the lost thermal stability, again reflecting the complementary nature of the side chains at positions 75 and 106. Since this pairwise interaction of Ala75 and Cys106 in *V. harveyi* luciferase parallels the conserved Gly75 and Val106 residues found in luciferases from the *Photobacterium* genus and *V. (Photobacterium) fischeri*, the results we present here further suggest that the structure of distant luciferase siblings is strongly conserved in three-dimensional space.

Luminescent Wavelength Spectrum. Flavin analogues with a modified isoalloxazine ring have been shown to yield different luminescent colors, providing good evidence that the isoalloxazine moiety is the chromophore producing the light emission (*28*). Using a continuous light-emitting assay developed to allow measurement of the bioluminescence spectrum "in vitro" (described in Experimental Procedures), we are able to readily measure changes in the emission spectra of 1 nm. Figure 4 shows that there is a red shift of ~8−10 nm in the emission spectrum of the C106V mutant and that this red shift is at least partly retained (~4 nm) in the A75G/C106V double mutant. The 8−10 nm red shift in the emission spectrum of the C106V mutant appears to be due at least in part to the conformational relaxation resulting from the overcrowding of Ala75 and Val106 side chains. The smaller red shift with the complementary pair of Val106 and Gly75 in the active site rather than Cys106 and Ala75 could arise from a slightly different conformation and the more apolar nature of Val106 compared to Cys106. Interestingly, the spectrum of the double mutant is very similar to that of *P. phosphoreum* luciferase, which is also red-shifted compared to the spectrum of the *V. harveyi* wild-type luciferase. In contrast, absolutely no difference in spectrum can be observed between the *Vh* wild-type luciferase and the A75G mutant (Figure 4). These results provide further support for the proposed geometry and location of the flavin mononucleotide as both the Ala74−Ala75 *cis*-peptide bond and Cys106 are in close contact with the chromophoric isoalloxazine ring (*4*). A disturbance in the microenvironment next to the isoalloxazine ring could readily cause a shift in the color of bioluminescence by perturbing the potential energy of the ground and/or excited state.

DISCUSSION

Impact of the C106V Mutation on Luciferase Structure and Function. Although the dark phenotypic properties (low specific activity, decreased level of aldehyde binding, and very rapid C4a-hydroperoxyflavin intermediate disintegration) of the single point mutant, C106V, are well-documented (*6*, *18*), the molecular basis for this loss of luminescence was not previously known at the atomic level. Properties like those of the wild type could be recovered for the luciferase mutant C106V by creating a double mutant, A75G/C106V, in which Ala75 is replaced with glycine. The results clearly demonstrate that the dark phenotype of C106V must arise from the unfavorable steric interaction between the side chains of Val106 and Ala75, which is the major cause for the debilitation in function. In addition to these results, the emission spectral red shifts in both the C106V (~8−10 nm) and C106V/A75G (~4 nm) mutants highlight the fact that the microenvironment engulfing the isoalloxazine ring is electronically different between luciferases carrying Val106 and those carrying Cys106, and support our proposed geometry of the flavin luciferase binary complex in which the isoalloxazine ring directly abuts the thiol group of Cys106

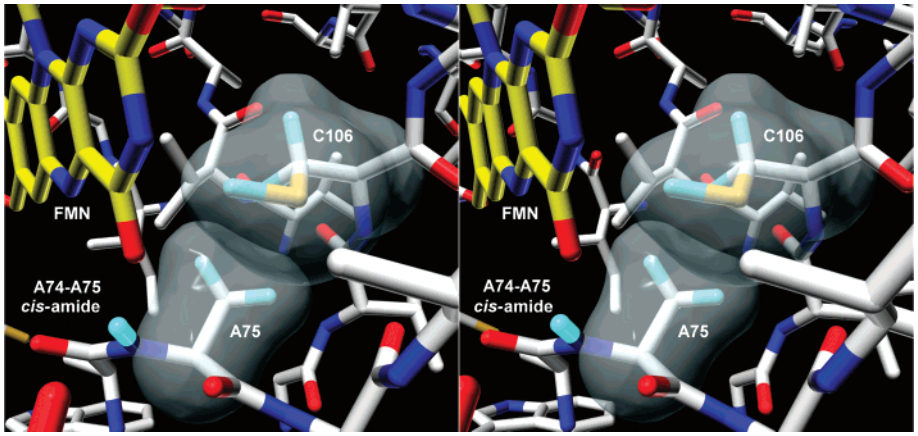

FIGURE 5: Stereoview of the proposed FMN isoalloxazine binding site. Molecular surfaces of Ala75 and Cys106 show the tight packing between the thiol group of Cys106 and the methyl side chain of Ala75. The isoalloxazine moiety of FMN binds directly above the *cis*-amide linkage of Ala74 and Ala75, and facing the thiol group of Cys106. Hydrogen atoms other than those of Ala75 and Cys106 were omitted for clarity.

(*4*). Five chemically induced *V. harveyi* luciferase mutants displaying various degrees of emission spectral red shifts have been isolated by Cline and Hastings (*29*); however, the site of mutation of only one mutant (D113N), originally designated as AK-6 (altered kinetic), with a 12 nm red shift in the emission spectrum, was identified (*7*, *9*). It may be relevant that Asp113 is only six residues away from position 106, and both Asp113 and Cys106 are flanking the β4−α4a loop (Cys106−Asp111), within which the backbone amide hydrogen of Leu109 establishes a hydrogen bond to the C2 carbonyl oxygen of isoalloxazine, a specific intermolecular interaction proposed in our binary complex model (4).

Figure 5 shows the close packing of the methyl side chain of Ala75 and the thiol side chain of Cys106 in the binary complex model of *V. harveyi* bacterial luciferase and flavin mononucleotide (*4*). Although the valine side chain could adopt a number of conformations around its rotatable Cα−Cβ bond, the impaired function of the C106V mutant suggests that none of those conformations is compatible with the structural environment of the wild-type luciferase. However, the rescue of function of the C106V mutant by the complementary A75G mutation reported here clearly indicates that one of the methyl groups in the Val106 side chain is accommodated in the same location that would otherwise be occupied by the methyl group of Ala75 in the structure of the wild-type luciferase (Figure 6). That is, the unfavorable steric repulsion between the side chains of Ala75 and Val106 in the C106V mutant would require a conformational change in the active site to relieve the steric overcrowding. The active site cavity in the luciferase structure is formed by the convergence of several loop structures (*1*), and the steric interaction between Ala75 and Val106 could directly affect the conformation of either or both the β3−α3 (Thr73−Pro83) and β4−α4a (Cys106−Asp111) loops. As the phosphate moiety of flavin mononucleotide is anchored via strong ionic contacts by the guanidinium group of Arg107 next to Cys106 on the β4−α4a loop (*3*, *4*), it would be expected that the binding of flavin would be seriously affected if this loop moved. However, the dissociation constant for $FMNH_2$ of the C106V mutant was the same as that for wild-type luciferase. This result is in agreement with our earlier finding of a broad

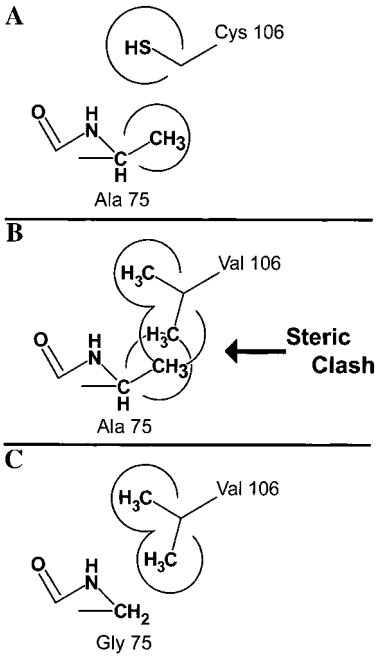

FIGURE 6: Schematic drawing describing the side chain steric interaction of positions 75 and 106 alongside the non-proline *cis*-peptide bond. (A) The methyl side chain of Ala75 is in the proximity of the sulfhydryl group of Cys106 such that two groups (encircled) fill the space alongside the Ala74−Ala75 *cis*-peptide bond. (B) Three methyl groups (encircled) from side chains of Ala75 and Val106 introduce a steric repulsion as the three groups collide. (C) By replacement of Ala75 with glycine, the unfavorable steric interaction is eliminated, thus allowing two methyl groups of valine (encircled) to fill the space next to the Ala74−Ala75 *cis*-peptide bond.

energetic minimum for accommodating the isoalloxazine ring in the active site cavity of luciferase (*4*). In that study, we relied on filtering a database of feasible bound flavin conformations by the structure−activity profile of flavin analogues to select the productive binding mode of the isoalloxazine ring. Thus, the conformational restriction imposed upon the productive binding of the flavin would not be reflected in the substrate affinity for the wild-type or mutant enzyme. Rather, this conformational selection would be manifested in the stability of the C4a-hydroperoxyflavin intermediate, resulting in the longevity of the intermediate being very sensitive to the particular isoalloxazine conforma-

tion. These results would suggest that not the β4−α4a loop but the β3−α3 loop containing the non-prolyl *cis*-peptide linkage between Ala74 and Ala75 may have moved in the C106V mutant to accommodate Ala75. This in turn would prevent the isoalloxazine ring from adopting the productive geometry in the C106V mutant, and hence would result in the decreased stability of the C4a-hydroperoxyflavin intermediate.

Potential Role of the Unusual Non-Prolyl Cis-Peptide Linkage. Our previous molecular modeling of the flavin location placed the catalytic isoalloxazine group immediately above the *cis*-peptide linkage between Ala74 and Ala75 on the β3−α3 loop (*4*). In particular, the C4 carbonyl oxygen and N5 hydrogen on the isoalloxazine could potentially form two hydrogen bonds with the amide NH and carbonyl oxygen of the *cis*-amide linkage between Ala74 and Ala75. Non-prolyl *cis*-peptide bonds are very special elements present at a very low frequency (0.03% of peptide bonds) in only a few proteins (*30*), with aliphatic amino acids (e.g., Ala) being the rarest of the substituents (*5*). The presence of these *cis*-bonds has often been associated with structural and/or functional purposes (*5*, *31*, *32*). When the non-prolyl *cis*-peptide linkage is present in the active site, the structurally bulged backbone amide can lead to the protrusion of the carbonyl oxygen and NH into the ligand-binding domain, allowing the *cis*-oriented carbonyl oxygen and NH to interact with ligands by functioning as a hydrogen bond acceptor and donor, respectively (*5*, *33*−*36*). Because of the close contact of the atoms projecting from the two Cα atoms of the amino acid residues linked by the *cis*-amide bond, the non-prolyl *cis*-amide bond is in a much higher energy state than the *trans*-amide bond (*37*). Entities with unusually high energy have often been associated with the ability to reach the transition state (*37*), and *cis*-bonds can facilitate reaction completion by discharging their potential energy by adapting a lower-energy conformation (i.e., *trans*-configuration) (*38*). Such a reaction-dependent non-prolyl peptide *cis*−*trans* isomerization has been demonstrated recently for concanavalin A (*39*) and *Clostridium beijerinckii* flavodoxin (*34*). It is of particular interest that the ligand of flavodoxin is also FMN, and the non-prolyl *cis*-bond in *C. beijerinckii* flavodoxin interconverts between different configurations to accommodate flavin in different oxidation states (*34*). Moreover, the non-prolyl *cis*-peptide bonds are located in similar positions in bacterial luciferase and *C. beijerinckii* flavodoxin relative to the isoalloxazine ring of FMN. However, in the case of *C. beijerinckii* flavodoxin, the carbonyl oxygen and the NH of the *cis*-peptide linkage are both oriented away from the isoalloxazine ring. Direct hydrogen bonding interaction occurs between the carbonyl oxygen of this peptide bond and the reduced flavin N5 hydrogen only when the peptide linkage is in the *trans*-configuration. In contrast, the carbonyl oxygen and NH of the Ala74−Ala75 bond in luciferase are proposed to hydrogen bond to the N5 hydrogen and C4 carbonyl oxygen of the isoalloxazine ring in only the *cis*-configuration. It is important to emphasize that both the functions and the three-dimensional structures of *C. beijerinckii* flavodoxin and bacterial luciferase are quite different even though both of their flavin binding sites contain non-prolyl *cis*-peptide bonds. Therefore, different modes of utilization of the non-prolyl *cis*-peptide bond in substrate binding and/or reaction catalysis would be expected.

These results, however, do clearly show that critical packing of side chains in the region near the unusual non-prolyl *cis*-peptide bond in luciferase is necessary to maintain the integrity and/or function of the active site and disruption of this packing could readily affect the interaction of the *cis*-bond with the isoalloxazine ring of flavin. Even a minor displacement of the *cis*-peptide bond would hinder flavin from adopting the correct active site binding geometry for a productive reaction via the light pathway, resulting in a loss of C4a-hydroperoxyflavin intermediate stability and aldehyde binding. Although the affinity for $FMNH_2$ did not change as the unfavorable steric interaction occurs at the proposed isoalloxazine binding site, a slight deviation in the proposed binding conformation would yield the unstable C4a-hydroperoxyflavin intermediate and consequently decreases the level of aldehyde consumption by the C106V mutant. Finally, it is indeed interesting to speculate that a *cis*-to-*trans* rotational module may also occur for bacterial luciferase as occurs in the concanavalin A and flaxodoxin systems (*34*, *39*).

REFERENCES

1. Fisher, A. J., Thompson, T. B., Thoden, J. B., Baldwin, T. O., and Rayment, I. (1996) *J. Biol. Chem. 271*, 21956−21968.
2. Fisher, A. J., Raushel, F. M., Baldwin, T. O., and Rayment, I. (1995) *Biochemistry 34*, 6581−6586.
3. Moore, C., Lei, B., and Tu, S. C. (1999) *Arch. Biochem. Biophys. 370*, 45−50.
4. Lin, L. Y., Sulea, T., Szittner, R., Vassilyev, V., Purisima, E. O., and Meighen, E. A. (2001) *Protein Sci. 10*, 1563−1571.
5. Jabs, A., Weiss, M. S., and Hilgenfeld, R. (1999) *J. Mol. Biol. 286*, 291−304.
6. Abu-Soud, H. M., Clark, A. C., Francisco, W. A., Baldwin, T. O., and Raushel, F. M. (1993) *J. Biol. Chem. 268*, 7699−7706.
7. Baldwin, T. O., Chen, L. H., Chlumsky, L. J., Devine, J. H., Johnston, T. C., Lin, J.-W., Sugihara, J., Waddle, J. J., and Ziegler, M. M. (1987) in *Flavins and Flavoproteins* (Edmondson, D. E., and McCormick, D. B., Eds.) pp 621−631, Walter de Gruyter & Co., Berlin.
8. Baldwin, T. O., Chen, L. H., Chlumsky, L. J., Devine, J. H., and Ziegler, M. M. (1989) *J. Biolumin. Chemilumin. 4*, 40−48.
9. Chlumsky, L. J., Chen, L. H., Clark, C., Abu-Soud, H., Ziegler, M. M., Raushel, F. M., and Baldwin, T. O. (1991) in *Flavins and Flavoproteins* (Curti, B., Ronchi, S., and Zanetti, G., Eds.) pp 261−264, Walter de Gruyter & Co., Berlin.
10. Francisco, W. A., Abu-Soud, H. M., DelMonte, A. J., Singleton, D. A., Baldwin, T. O., and Raushel, F. M. (1998) *Biochemistry 37*, 2596−2606.
11. Fried, A., and Tu, S. C. (1984) *J. Biol. Chem. 259*, 10754−10759.
12. Lei, B., Cho, K. W., and Tu, S. C. (1994) *J. Biol. Chem. 269*, 5612−5618.
13. Merritt, M. V., and Baldwin, T. O. (1980) *Arch. Biochem. Biophys. 202*, 499−506.
14. Nicoli, M. Z., Meighen, E. A., and Hastings, J. W. (1974) *J. Biol. Chem. 249*, 2385−2392.
15. Nicoli, M. Z., and Hastings, J. W. (1974) *J. Biol. Chem. 249*, 2393−2396.
16. Paquatte, O., Fried, A., and Tu, S. C. (1988) *Arch. Biochem. Biophys. 264*, 392−399.
17. Paquatte, O., and Tu, S. C. (1989) *Photochem. Photobiol. 50*, 817−825.
18. Xi, L., Cho, K. W., Herndon, M. E., and Tu, S. C. (1990) *J. Biol. Chem. 265*, 4200−4203.
19. Meighen, E. A. (1991) *Microbiol. Rev. 55*, 123−142.
20. Hastings, J. W., Baldwin, T. O., and Nicoli, M. Z. (1978) *Methods Enzymol. 57*, 135−152.
21. Gunsalus-Miguel, A., Meighen, E. A., Nicoli, M. Z., Nealson, K. H., and Hastings, J. W. (1972) *J. Biol. Chem. 247*, 398−404.
22. Gill, S. C., and von Hippel, P. H. (1989) *Anal. Biochem. 182*, 319−326.

23. Meighen, E. A., and Hastings, J. W. (1971) *J. Biol. Chem. 246*, 7666−7674.
24. Meighen, E. A., and MacKenzie, R. E. (1973) *Biochemistry 12*, 1482−1491.
25. Hastings, J. W., and Gibson, Q. H. (1963) *J. Biol. Chem. 238*, 2537−2554.
26. Francisco, W. A., Abu-Soud, H. M., Baldwin, T. O., and Raushel, F. M. (1993) *J. Biol. Chem. 268*, 24734−24741.
27. Holzman, T. F., and Baldwin, T. O. (1983) *Biochemistry 22*, 2838−2846.
28. Mitchell, G., and Hastings, J. W. (1969) *J. Biol. Chem. 244*, 2572−2576.
29. Cline, T. W., and Hastings, J. W. (1974) *J. Biol. Chem. 249*, 4668−4669.
30. Tochio, H., Ohki, S., Zhang, Q., Li, M., and Zhang, M. (1998) *Nat. Struct. Biol. 5*, 965−969.
31. Ramachandran, G. N., and Mitra, A. K. (1976) *J. Mol. Biol. 107*, 85−92.
32. Stewart, D. E., Sarkar, A., and Wampler, J. E. (1990) *J. Mol. Biol. 214*, 253−260.
33. Cody, V., Galitsky, N., Rak, D., Luft, J. R., Pangborn, W., and Queener, S. F. (1999) *Biochemistry 38*, 4303−4312.
34. Ludwig, M. L., Pattridge, K. A., Metzger, A. L., Dixon, M. M., Eren, M., Feng, Y., and Swenson, R. P. (1997) *Biochemistry 36*, 1259−1280.
35. Shi, W., Tanaka, K. S., Crother, T. R., Taylor, M. W., Almo, S. C., and Schramm, V. L. (2001) *Biochemistry 40*, 10800−10809.
36. Zajc, A., Romao, M. J., Turk, B., and Huber, R. (1996) *J. Mol. Biol. 263*, 269−283.
37. Herzberg, O., and Moult, J. (1991) *Proteins 11*, 223−229.
38. Stoddard, B. L., and Pietrokovski, S. (1998) *Nat. Struct. Biol. 5*, 3−5.
39. Bouckaert, J., Dewallef, Y., Poortmans, F., Wyns, L., and Loris, R. (2000) *J. Biol. Chem. 275*, 19778−19787.

BI020295O